

Efficiency and durability of protective treatments on cultural heritage copper corrosion layers

Emilande Apchain^{a,b,*}, Delphine Neff^a, Jean-Paul Gallien^a, Nicolas Nuns^c, Pascal Berger^d, Albert Noumowé^b, Philippe Dillmann^a

^a LAPA-IRAMAT, NIMBE, CEA, CNRS, Université Paris-Saclay, CEA Saclay, Gif-Sur-Yvette Cedex, France

^b L2MGC, Université de Cergy-Pontoise, Neuville-sur-Oise, France

^c Univ. Lille, CNRS, INRA, Centrale Lille, ENSCL, Univ. Artois, FR 2638 - IMEC - Institut Michel-Eugène Chevreul, F-59000 Lille, France

^d LEEL, NIMBE, CEA, CNRS, Université Paris-Saclay, CEA Saclay, Gif sur Yvette Cedex, France

*Corresponding author. Tel.: +33-1-34-25-70-71

Postal address: L2MGC, Université de Cergy-Pontoise,

5 mail Gay Lussac, F-95031 Neuville-sur-Oise, France

Email address: emilande.apchain@cyu.fr

Abstract

To protect copper artefacts of the cultural heritage from atmospheric degradation protective treatment must be applied. Two types of protective treatments: microcrystalline wax (Cosmolloïd wax) and decanoate solution (HC₁₀) were tested. Two aspects were considered: the penetration of the treatments in the corrosion layers, and its durability. Equivalent efficiencies for both treatments were demonstrated. The penetration of the treatments seems to depend essentially on its application mode. Re-corrosion experiments of treated samples under immersion in D₂O demonstrate that the efficiency and the durability with time or after water leaching depend on the penetration of the treatments in the corrosion layers.

Keywords: copper; copper alloys; atmospheric corrosion; protective treatments; microcrystalline wax; decanoate solution

1. Introduction

In outdoor environment, copper and copper based alloys (e.g. bronzes) undergo degradations mainly caused by water (rain, moisture) but also related to air pollution [1–3]. Consequently, for cultural heritage artefacts and work of art made of these alloys and exposed outdoor, the understanding of these degradation processes but also the choice of adapted protection treatments is of crucial importance [4,5]. Actually, the atmospheric corrosion of the statues and work of art leads to the formation of a corrosion layer, and consequently the modification of the aesthetic aspect of the work. The corrosion layer, also called patina for bronze artwork [6], is known to be formed through a two-stage process in the case of pure copper [7–11] and bronze [12–18].

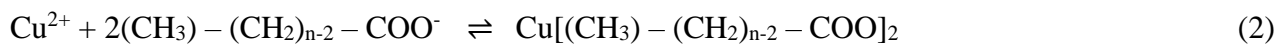
For unalloyed copper it is well known that a thin layer of brownish cuprite (Cu_2O) is at first formed on the metal. Then, progressively an electrolyte film forms on the surface of the cuprite layer, containing different species, depending on the environment, among which the most common are sulfate and chloride. The outer part of the cuprite dissolves and this process induces, after an oxidation of Cu(I) into Cu(II) species, the precipitation of an outer layer which gives a characteristic greenish color to the surface composed of Cu(II) species. In an urban or industrial environment this green layer is mainly composed of brochantite $\text{Cu}_4\text{SO}_4(\text{OH})_6$ [19]. In an industrial environment the more acidic conditions tend to induce the precipitation of antlerite, another copper hydroxysulfate $\text{Cu}_3(\text{OH})_4\text{SO}_4$ [20]. In a marine environment the main constituents of the corrosion layer are an inner thin layer of cuprite and a thicker mixed layer of atacamite $\text{Cu}_2\text{Cl}(\text{OH})_3$ and paratacamite $\text{Cu}_3(\text{Cu, Zn})\text{Cl}_2(\text{OH})_3$ [7,8]. Concerning bronze alloys the presence of tin and lead in the metallic matrix introduces a slightly different corrosion mechanism as proposed by Robbiola et al. [1]. These authors have shown that insoluble tin oxides precipitate inside the corrosion layer and act as a cathode for the copper matrix. This induces the selective dissolution of the metallic copper, the solid diffusion of copper (I) through the corrosion layer and their precipitation as copper (II) phases on the outer part of the corrosion layer.

Whatever the metallic matrix is, the presence of corrosion layers causes a decrease of the corrosion rate (CR). The CR is a sensitive function of relative humidity, sulfur dioxide, hydrogen sulfide, ozone, hydrogen chloride, and chlorine concentrations [21,22] but it starts to decrease while a 5 nanometer thick cuprite layer is formed [9]. Cuprite is a semiconductor phase that controls the oxidation rate through the limitation of the diffusion of Cu(I) species produced by the anodic reaction. Whatever the environment is, the CR also decreases with the exposure time [8,23]. This decrease is abrupt over the first 3–4 years, especially in the marine atmospheres. It becomes more gradual for longer periods, but is still not stabilized after 13 to 16 years of exposure [8].

Even though the cuprite layer can have a protective effect, the continuous degradation of the external porous layer induces a penetration of the water through the corrosion layer until the cuprite layer that tends to dissolve progressively. Moreover the runoff occurring on samples exposed outdoor induces the leaching of the corrosion layer which is harmful for the preservation of ancient artefacts [7]. Therefore, the restoration treatment based on the reinforcement of the protectiveness of this layer is mandatory for the preservation of the cultural heritage outdoor artefacts. As far as cultural heritage is concerned, protection treatments must meet some requirements. To be used by conservators, the treatment must respect the original aesthetics of the artefact and allow future interventions. Transparent and soluble products in various solvents are then required. Two types of protective treatments are currently used in the field of cultural heritage: microcrystalline waxes and corrosion inhibitors [24]. Today in France, the most currently used treatment for outdoor exposure is the microcrystalline wax. These synthetic waxes made of saturated hydrocarbons with long chains [25–32] make a physical barrier on the object surface. These treatments offer the best compromise between efficiency and aesthetic aspect [25,27,30–32]. Some works highlighted the influence of the nature of the corrosion layers [31,32] and of the application mode on the treatment efficiency [33]. Nevertheless, the durability of these treatments is relatively limited [30,32] and dusting problems were noted [34]. Therefore, the protected surfaces require regular applications, ideally every year, but this upkeep costs a lot and is not always implemented as regularly as required.

Other protection treatments are considered for years to inhibit the corrosion phenomena. Corrosion inhibitors act by forming a new compound by reaction with the substrate to slow down the corrosion process. These compounds were generally tested and applied directly on metallic surfaces in the industrial field. Moreover, they are developed originally for metallic pieces immersed in an aqueous solution. Nevertheless, their use has been transposed to the field of metallic heritage protection. For copper based alloys benzotriazole (BTA) and derivatives are mainly used as corrosion inhibitors in the field of cultural heritage [35]. In France corrosion inhibitors are essentially used for small metallic artefacts, generally from archaeological origin, and stored in indoor conditions. In Italy, mixed systems with Incralac and microcrystalline wax are used on objects submitted to outdoor exposure. However, the question about the possible toxicity of BTA is raised by some studies [36,37]. Therefore, for several years work has focused on the development of “green” corrosion inhibitors [38,39]. In particular new formulations of corrosion inhibitors have been developed based on carboxylate solutions $\text{CH}_3(\text{CH}_2)_{n-2}\text{COO}^-(\text{Na}^+, \text{H}^+)$, abbreviated to HC_n or NaC_n . These non-toxic and non-carcinogen compounds derived from fatty acids extracted from vegetable oil (colza, sunflower, and palm) conduct to the formation of a protective layer composed by a metal-carboxylate complex, by reacting with metallic ions [40–42]. The protective mechanism on non-

corroded occurs in two steps: the oxidation of copper in solution following Eq. (1) and the reaction of Cu^{2+} ions with carboxylate anions following Eq. (2).



The protection of treated copper is due to the formation of a thin layer of metallic soap conferring a hydrophobic property to the surface [42]. But in the case of ancient copper artefacts, a corrosion layer is present which cannot be removed because it is part of the history of the artefact.

Several studies have been conducted on the global efficiency of these treatments on various metals. The Promet project was a European Project from 2004 to 2008 “Developing new analytical techniques and materials for monitoring and protecting metal artefacts and monuments from the Mediterranean region” [43]. As part of this project, the corrosion inhibiting effects of several carboxylates solutions have been studied on bare and corroded iron [44]. Electrochemical analyzes have highlighted the inhibiting effect of NaC_{10} and HC_{10} solution on both bare and corroded iron, but with a less effective protection for the NaC_{10} solution. Indeed, in basic medium the carboxylate film does not exceed one micron thick while the treatment with acid carboxylate solutions allows the growth of relatively thick passivating layers (about several micrometers thick). Decanoic acid has also been tested on a sea anchor from the Musée National de la Marine in Paris. After 9 months of natural aging (storage conditions without controlled atmosphere) only the untreated part of the object shows corrosive recoveries, confirming the efficiency of this treatment [39]. In 2012 tests with decanoate solutions (NaC_{10} and HC_{10}) have been carried out on a several decades corroded steel. After 5 days of immersion in the carboxylate treatment solution, the samples were immersed in a corrosive medium [45]. Electrochemical impedance spectroscopy analyzes have shown the anodic inhibitory action of carboxylates, but this study also highlights the less protective effect of NaC_{10} .

Regarding copper protection several studies have shown the efficiency of sodium carboxylate solutions on bare copper [42,46,47]. Some studies have also studied the protective effect of carboxylate solutions in acid form [48]. As early as 1996 electrochemical analyzes showed that a maximum of efficiency against corrosion was obtained, on non-corroded copper, after an immersion in a solution of NaC_7 at pH 8 due to the formation of a $\text{Cu}(\text{C}_7)_2$ film on the copper surface [42]. Regarding the protection of corroded copper or copper alloys, very little work has been carried out [40].

Although several studies have been carried out on non-corroded metals, very little has been done on corroded copper and particularly on the penetration of the treatment in the corrosion layers, linked

to its durability. So far, most studies aiming the protectiveness of the treatments are based on electrochemical analyzes, giving information about the efficiency of protective treatments but none about the interactions at microscopic scale with the substrate. The protection mechanism and the treatment efficiency when carboxylate solution has been applied on an already corroded surface remain unknown as well as a possible penetration of this treatment in the corrosion product layer. Furthermore, all these studies concern essentially one type of treatment at once and only in their short-term effectiveness, without considering neither the climatic effects on their durability nor the effect of the application mode. In this study a new and complementary approach is proposed, based on the use of isotopic markers in corrosive media associated with isotopic analysis techniques. Our aim is here to compare the protection mechanisms (especially the penetration in the corroded layer) and the durability under different chemical solicitations of a usual treatment already used in the restoration field (microcrystalline wax) and a carboxylate one, the decanoic acid.

For the microcrystalline wax we chose to work with the Cosmolloïd wax that seems to have the best efficiency compared to other microcrystalline waxes in the context of the protection of naturally weathered copper [49]. Regarding the carboxylate solution the decanoic acid that showed the best results on non-corroded iron [44] was selected.

2. Materials and methods

2.1. Treatments on ancient samples

The study was conducted on samples from copper sheets deposited from the roof of the St Martin church in Metz (France) after about 130 years of exposure. Its microstructure is made of equiaxed grains of about several tenth micrometers (Figure 1). The corrosion layer of this copper roof formed naturally during the outdoor exposition. It presents a greenish surface color. The experiments were performed on samples of about 1 cm² that were cut from the roofing sheet.

Two protection treatments were applied in this study: microcrystalline wax classically used by restorers and a carboxylate solution. The microcrystalline wax was the commercial Cosmolloïd wax which is one of the most commonly used by restorers. Cosmolloïd wax solution diluted in White Spirit solvent has been applied to copper samples by a restorer of the Laboratoire de Recherche des Monuments Historiques (LRMH), in two different ways [49], following the most common application modes used by conservators in France:

- A so-called “hot” application: during the application of the wax with a brush the substrate was heated at approximately 60°C. The heating was stopped at the end of the application, when the corrosion layer is considered as saturated by visual inspection. The wax was then dried for 24 hours and lustrated with a soft brush.

- A so-called “cold” application: the substrate was heated at about 60°C to dry the surface and possibly remove the water from the pores of the corrosion layers. Then the heating was stopped, and a first layer of wax was applied. A second layer of wax was then applied after 24 hours of drying at ambient temperature. After a last drying step of 24 hours, the wax was lustrated with a soft brush.

For the carboxylate treatment, a decanoic acid solution (0.17 M) was prepared by dissolving 3 g of decanoic acid (Sigma Aldrich) in a mixture of 50 mL of water and 50 mL of ethanol. The decanoic acid solution was applied on the samples using two different application modes:

- with a brush, two coats with a drying time of one hour between the two applications
- by immersion for 1, 5, 30 minutes and for 1, 2 and 3 hours

To follow the penetration of the decanoate inside the corrosion layer even for low quantities, specific experiments using carbon-13 were also conducted. The same treatment protocols were applied as described above but with a solution of carbon-13 doped decanoic acid marked at 10%. The labelled carbon corresponds to the one of the carboxylate group. The ¹³C treatment also allowed us to differentiate the carbon from the treatment and the carbon from the coating resin added during the sample preparation step to detect the carboxylate compound penetration inside the corrosion layer, especially for the samples immersed in the decanoic acid solution at shorter duration. ¹³C detection was done by nuclear reaction analyses as detailed below.

After all treatments, the samples were dried in an oven at 80°C for 12 hours.

Only a small part of 0.5 cm² from the treated sample center is studied afterwards. According to the orders of magnitude of the diffusion coefficients of liquids in porous media (10^{-11} m²/s – 10^{-8} m²/s [50]) the solution would penetrate between 0,03 cm and 0,85 cm into the corrosion product layer after 2h of immersion. This estimates shows that the complexants observed in the middle of the sample plate can't have penetrated from the cut sides of the sample.

2.2. Leaching and recorrosion experiments

To simulate the exposition to rainfall a device was developed to drop water on the surface of the samples inclined at 45°. The flow rate was set to simulate an equivalent volume of two years of

rainfall in Paris (Météo France Data) during a period of 7 days. Thus, 20.16 L of distilled water, with a flow rate of 0.12 L/h was dropped on each sample surface of 1 cm².

However, the leaching simulation was accelerated and the study was essentially qualitative, not taking into account the intensity of the accelerated leaching or the time of wetness. The observations will not allow quantifying the durability of both treatments and the application modes under a leaching stress.

To evaluate the efficiency of the protective treatments to act as liquid water repellent, the samples were immersed in deuterated water (D₂O). The experiments were conducted as follows. First the samples were coated on each side by a polyurethane resin to leave accessible to the solution only the top surface of the corrosion layer. Then samples were immersed during 1 and 4 months in a deuterated water solution at ambient conditions. After immersion, the samples were re-embedded in an epoxy resin and prepared on transverse sections following the protocol presented below. On cross section, the amount of residual deuterium was detected by ToF-SIMS (Time of Flight Secondary Ions Mass Spectrometry) in the corrosion layers (see next section).

2.3. Analytical protocols

For all the analytical techniques, the samples were prepared on cross section. The results presented below are reproducible since several analyzes on each sample were made at several areas of the cross section. The corrosion product layout is similar throughout the cross section so the data obtained after treatment can be compared with each other.

The untreated sample was directly embedded in an epoxy resin. Concerning the treated samples they were wrapped in a thin tin foil before embedding to limit the penetration of resin into the corrosion layer. All transverse sections were cut with a diamond saw and then polished using silicon carbide abrasive papers (SiC, from grad 320 to 4000) and diamond suspensions (3 and 1 μm).

After observations under Optical Microscopy, morphology and chemical composition of the samples were studied thanks to SEM-EDS analyses (scanning electron microscope coupled to energy dispersive spectroscopy) using a field emission gun scanning electron microscope (FEG-SEM) JEOL-LSM-7001F. The cross sections were previously coated with a thin carbon layer (~ 20 nm thick) to avoid the accumulation of charges on the non-conductive phases. The FEG-SEM is coupled to an EDS SDD (Silicon Drift Detector) detector Oxford for the chemical composition analyses. The analyses were performed at a voltage of 15 kV. Maps of the chemical elements constitutive of the

corrosion layers were also recorded to determine the distribution of the different elements constituting the corrosion layers.

For the identification of the crystalline structure of the corrosion layers μ Raman spectroscopy analyses were performed using a Renishaw InVia spectrometer. It is equipped with a frequency doubled Nd:YAG laser emitting at 532 nm. A Leica LM/DM (x50) microscope was used to focus the laser on the sample with a beam diameter of about 1.5 μ m. The laser power did not exceed 100 μ W in order to avoid the transformation of the phases by heating. The spectral resolution is of the order of 2 cm^{-1} . For the identification of the phases spectra were either compared to data available in the literature or acquired on the laboratory set-up on synthesized phases. Cuprite and decanoic acid were purchased from Sigma Aldrich, brochantite was synthesized following the Kratschmer et al. protocol [51] and copper decanoate was synthesized following the Robinet et al. protocol [52]. Maps analyses were also performed to show the distribution of the phases inside the corrosion layers. The phase distribution was done by extracting the peak area of a representative peak (Region Of Interest ROI) for each phase and a color intensity map was established. The data were recorded and processed with the Wire software. As all the Raman reference spectra required for this study are not available in the literature, on-site acquisitions on the spectrometer were performed.

For the marked ^{13}C experiments described previously, the penetration of the ^{13}C doped decanoate inside the corrosion layer was detected by nuclear reaction on a nuclear microprobe facility (NIMBE/LEEL laboratory, France). This microprobe is equipped with a single-stage Van de Graaf electrostatic accelerator (KN-3750 from HVEC) [53,54]. The analysis of ^{13}C is based on the detection of the protons emitted by the nuclear reaction induced by the interaction of ^{13}C nuclei and a deuteron beam as expressed by the formula $^{13}\text{C}(\text{d},\text{p})^{14}\text{C}$. The energy of the incident beam of deuterons was set at 1.40 MeV to benefit from a high cross-section of this nuclear reaction and the focusing of the beam through magnetic lens allowed to obtain a beam size of approximately 3 x 3 μm^2 . The annular detector was set to collect emitted particles at a detection angle of 170°. The resulting spectrum obtained for each sample is the sum of the whole pixel spectra corresponding to the corrosion layer. The obtained experimental spectra show also signals from $^{12}\text{C}(\text{d},\text{p})^{13}\text{C}$ nuclear reaction and from backscattered deuterons on heavier elements. They were then simulated using the SIMNRA software after providing the experimental data information (beam energy, setup geometry, interaction cross-sections, stoichiometry of the studied area, thickness, etc.) to support the calculation [55]. The adjustment of the experimental and simulated data ensures the determination of the isotopic ratio $\left(\frac{^{12}\text{C}}{^{13}\text{C}}\right)$.

From these values an enrichment factor relative to the untreated sample was calculated for each treated sample using the following formula:

$$\delta^{13}\text{C} = 100 \times \left[\frac{\left(\frac{^{12}\text{C}}{^{13}\text{C}}\right)_n}{\left(\frac{^{12}\text{C}}{^{13}\text{C}}\right)_0} - 1 \right]$$

with $\left(\frac{^{12}\text{C}}{^{13}\text{C}}\right)_n$ and $\left(\frac{^{12}\text{C}}{^{13}\text{C}}\right)_0$ the isotopic ratio $\left(\frac{^{12}\text{C}}{^{13}\text{C}}\right)$ of the treated (n) and untreated (0) samples.

To evaluate the efficiency of the treatments to repeal the water penetration in the corrosion layer after the deuterated water immersions deuterium enrichment was measured by ToF-SIMS. ToF-SIMS analyzes were conducted on a TOF.SIMS 5 device from IONTOF® and the acquisition was done using the Surface Lab® software. Given the composition of the different phases in the corrosion layers the negative polarity was preferred for these analyzes. Mappings were performed on the zones of interest in order to get the local distribution of the elements. The zones of interest selected by SEM prior to the ToF-SIMS analyzes were first etched with a Cs⁺ ion beam of 2 keV over an area of 800 μm x 800 μm (a few hundred nanometers thick) to remove the surface pollutants, and particularly the accumulation of hydrogen on the surface. Then an incident Bi⁺ primary ion beam scanned an area of 100 μm x 100 μm. For each sample an acquisition of 200 scans was made, each scan resulting from a cycle of 512 x 512 pulses of Bi⁺, an abrasion of 2 seconds and a pause of 0.5 seconds. Because the analyzed phases were not sufficiently conductive, an electron gun (or “floodgun”) was used during the acquisition to facilitate the discharge of charges. Due to matrix effect, making quantification by ToF-SIMS very difficult, we achieved a semi-quantitative approach consisting, not in considering the evolution of the deuterium intensity alone but of the D/H ratio in the brochantite zone. Nevertheless, an isobaric interference has to be considered. To distinguish the deuterium peak and the dihydrogen peak a minimum mass resolution R_{min} is necessary. R_{min} is defined as follows:

$$R_{\min} = \frac{m}{\Delta m} = \frac{m(\text{D})}{m(\text{D})-m(\text{H}_2)} \approx 1130$$

with m(D) and m(H₂) respectively the mass of deuterium and dihydrogen.

The burst alignment mode does not seem to have a sufficient mass resolution ($m/\Delta m \approx 200$) to allow the separation of these two peaks. However, the first analyzes in bunch mode have shown a systematic saturation of hydrogen’s signal which has led to an over-evaluation of the D/H ratio.

Therefore, it has been chosen to use burst alignment mode, and to limit the presence of dihydrogen on the samples related to the surface contamination thanks to the Cs⁺ abrasion carried out during the analysis. On the other hand, the bunch mode showed that during our measurements in non-interlaced mode, the proportion of H₂⁻ was very low and could perfectly be neglected in our isotope ratio calculations. Last the recombination of hydrogen coming from the OH of brochantite, has been estimated to be negligible thanks to a measurement on non-weathered samples. Indeed, the D/H ratio of such sample corresponds to the natural abundance (0.015%), discarding any isobaric interferences.

The mass spectra corresponding to the brochantite zone in the corrosion layer were recalculated thanks to the sum of spectra selected from the distribution maps of sulfur. The peak areas corresponding to the m/z of deuterium and hydrogen were then recorded. From these areas a deuterium and hydrogen ratio R could be calculated:

$$R = \frac{N_D}{N_H}$$

with N_D and N_H the number of counts detected for deuterium and hydrogen.

The enrichment factor was calculated relative to the untreated and unimmersed sample with the following formula:

$$\delta_D = 100 \times \left[\frac{\left(\frac{D}{H}\right)_n}{\left(\frac{D}{H}\right)_0} - 1 \right]$$

with $\left(\frac{D}{H}\right)_n$ the ratio of the intensities of D and H of the immersed samples and $\left(\frac{D}{H}\right)_0$ the ratio of intensities of D and H of the unimmersed sample

The results presented below are representative since several analyzes on different areas of each cross sections were made.

3. Results and discussion

3.1. Reference analyses for Raman spectroscopy

Pellets of reference phases have been analyzed by Raman spectrometry and average spectra were obtained from ten acquisitions (Figure 2). The Raman spectrum obtained on the synthesized brochantite shows a high intensity peak around 972 cm⁻¹ corresponding to the symmetrical

elongation of the S-O bond. Regarding the spectrum of cuprite, a main peak at 216 cm^{-1} is observed and attributed to the Cu-O bond. The Raman spectrum of Cosmolloid wax shows a series of peaks between 1300 and 3000 cm^{-1} attributed to the deformation of the CH_2 bonds [56], while peaks at 1061 and 1131 cm^{-1} are attributed to the elongation of the C-C and C-O bonds. The spectrum of copper decanoate shows a series of peaks between 1200 cm^{-1} and 3000 cm^{-1} attributed to the deformations of the CH_2 bonds, and another series between 1000 cm^{-1} and 1200 cm^{-1} corresponding to the deformation of the C-C bonds. Finally, the peaks observed between 230 cm^{-1} and 400 cm^{-1} are attributed to the deformations of the Cu-O bonds.

The superposition of the Raman spectra of brochantite and cuprite allows the identification of each phase characteristic and distinctive peaks: at 218 cm^{-1} for cuprite and 972 cm^{-1} for brochantite. The superposition of these phases' spectra with the Cosmolloid wax and the copper decanoate shows distinctive peaks at 1061 and 1131 cm^{-1} for the wax and 290 cm^{-1} for the copper decanoate. These peaks will allow us to map the distribution of these latter phases in the corrosion products.

3.2.Characterization of the untreated corrosion system

The elementary mappings made by SEM-EDS and Raman spectroscopy investigations shows compositional and structural differences between the inner and the outer corrosion products layer (Figure 3). The inner layer is composed of copper and oxygen. Their content are in good agreement with the elementary composition of cuprite Cu_2O (copper 89 %wt and oxygen 11 %wt). The Raman spectrum gathered at this location confirms the presence of this phase (Figure 4b). The outer layer is made of copper, oxygen and sulfur. Their content are close to the one of brochantite $\text{Cu}_4\text{SO}_4(\text{OH})_6$ (copper 55 %wt, oxygen 35 %wt and sulfur 10 %wt) which presence is confirmed by μ Raman analyses (Figure 4c).

This general layout is the same throughout the cross section and corresponds to the one already identified by numerous studies made on long term atmospheric corrosion of copper [7–9,19,57,58]. Overall, the average thickness of the whole layer is of $55\text{ }\mu\text{m}$ including a brochantite layer thickness of about $50\text{ }\mu\text{m}$ and a cuprite one of $4\text{--}5\text{ }\mu\text{m}$ in average, with thicknesses homogeneous throughout the sample (Figure 5).The comparison of the respective thicknesses of the cuprite and the brochantite layers have been studied on samples exposed from two to 142 years in various sites under different atmospheric conditions [7]. The authors deduced from these observations that the kinetic of formation of the cuprite is stabilized after about 15 years of corrosion. As the kinetic of dissolution of the metal and of the external part of the cuprite are equivalent, the thickness of the cuprite is then

stabilized to few micrometers. The brochantite thickness however is variable depending on the environment and on the run-off effect [59], making impossible to link it to time of exposure.

A slight enrichment of chlorine is observed locally in the corrosion layer. The elementary X ray maps (Figure 3) suggest that this element is located at the interface between the brochantite and the cuprite layer. Quantitative analyzes were obtained from the average spectra extracted from the different zones (Table 1). Even locally, the amount of chlorine is lower than the stoichiometry of the chlorinated phases most often observed in the corrosion products layers formed in atmospheric conditions (nantokite CuCl and atacamite $\text{Cu}_2\text{Cl}(\text{OH})_3$). Few studies mention the presence of chlorine on the outermost corrosion layer for samples exposed to marine environment [7, 50]. Only one study identified nantokite. Contrary to our study this phase is located between the metal and the cuprite layer [8]. In our study, it was not possible to get a different Raman signal than the one of pure brochantite in the Cl-containing zone. This supports the fact that the relative low Cl amounts is linked to a low but regular quantity of Cl containing phases mixed with brochantite or the presence of weakly crystallized phases.

Table 1: EDX compositions of the corrosion layers of the Metz sample:

	Cuprite	Brochantite	Nantokite	Atacamite	Inner layer	Outer layer	Chlorinated zones
	% wt						
Cu	89	56	64	60	91	59	63
O	11	35	-	22	9	31	26
S	-	7	-	-	-	9	5
Cl	-	-	36	17	-	-	3

3.3. Characterization of the treated corrosion layers

μ Raman investigations carried out on the sample treated with Cosmolloid wax are presented on Figure 6. The peak positioned at 1061 cm^{-1} was used to map the distribution of the wax on the transverse section. Results show a penetration of the wax depending on the application mode. For the “hot” application the presence of wax is detected inside the brochantite layer, up to the interface with the cuprite layer. The concentration of wax is however much higher in the outer part of the brochantite layer of about $20\text{ }\mu\text{m}$ thick. In contrast, no signal of the wax was detected in the cuprite layer (Figure 6a). For the “cold” application, a wax layer of about $10\text{-}15\text{ }\mu\text{m}$ thickness is evidenced

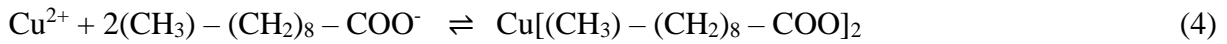
on the outer part of the corrosion layer. No wax is detected in the layer of cuprite or inside the inner part of the layer of brochantite (Figure 6b). The fact that the substrate was heated only prior to the application of the wax implies probably a quick decrease of the temperature of the substrate (melting point of wax: about 80°C [60]) and, consequently, a higher viscosity of the wax, hindering its penetration in the microscopic pore network of the corrosion layer. At the contrary, in the case of the “hot” application, the constant heating of the substrate during the application was performed until the substrate was saturated thus causing a softening of the wax. This leads probably to a decrease of the wax viscosity and therefore a difference of its penetration depth in a porous material.

For the sample treated by applying two coatings of decanoic acid by brush (Figure 7a) as well as for samples treated by immersion during 1 to 30 minutes (results not shown) μ Raman spectroscopy does not evidence any peak of copper decanoate in the corrosion product layers. On the contrary, after 1 hour of immersion in decanoic acid, the characteristic peak of copper decanoate at 290 cm^{-1} is observed in the whole thickness of the brochantite layer, but not in the cuprite (Figure 7b). The low intensity of this peak shows however that the copper decanoate is mixed with brochantite. Last, regarding the treatment by immersion for 3 hours in decanoic acid, μ Raman mapping shows that almost the whole outer layer of brochantite is converted into copper decanoate (Figure 7c).

The results of the $\delta^{13}\text{C}$ enrichment versus the type and duration of the treatment are reported on Figure 8. A carbon-13 enrichment ($\delta^{13}\text{C}$) of about 5% is detected on the sample treated by brush application although a weak $\delta^{13}\text{C}$. Concerning the immersion treatment, the sample immersed one minute shows a $\delta^{13}\text{C}$ enrichment of about 50%. Compared to the brushed sample, this suggests a better penetration of the decanoic acid by immersion. While increasing the immersion duration, $\delta^{13}\text{C}$ enrichment keeps increasing, to reach 500 % after 2 hours of immersion. Nevertheless, the graph of Figure 8 shows a plateau after 30 minutes of immersion. This stabilization may be due to a relative saturation of the corrosion layer after 30 minutes.

The comparison between the results obtained with the ^{13}C experiments and the Raman analyses are interesting. When the decanoic acid is applied by brush, μ Raman did not allow us to detect any signal in the layer. On the contrary NRA analyses on ^{13}C doped compounds reveal a relatively weak $\delta^{13}\text{C}$ enrichment compared to the one measured after at least 1-hour immersion. Thus, it seems that only very small amounts of HC_{10} penetrate in the corrosion layer while samples are treated by brush or by short immersion. At the contrary, the penetration in the corrosion layer of the decanoic acid during longer immersion times is attested both by μ Raman spectroscopy and ^{13}C NRA profiles. This penetration depends on the duration and the layer seems to be saturated after 120 minutes of immersion. Moreover after 30 minutes the penetrated HC_{10} quantity is significant.

The efficiency of the carboxylate within the corrosion layer could be related to the penetration of the HC₁₀ but also to the conversion of brochantite to copper decanoate. This conversion occurs in two stages: the dissolution of brochantite in acid media following Eq. (3) and the reaction of Cu²⁺ ions from brochantite with decanoate ions following Eq. (4).



Indeed, copper decanoate being hydrophobic, the conversion of the brochantite layer would highly limit water penetration. This conversion is attested by the presence of the peak at 290 cm⁻¹, typical of Cu(C₁₀)₂ on the Raman spectra when present. This peak was observed at the surface of all the samples treated by brush or by immersion attesting of the conversion of the top layer for all the treatments (results not shown in this paper). Inside the corrosion layer, the copper carboxylate was observed by μ Raman spectroscopy only after relatively long immersion times (1h and 3h) and throughout the whole cross section. Nevertheless, the penetration of HC₁₀ for shorter immersion times, observed by following ¹³C doped compounds, suggests that it is highly probable that copper carboxylate forms inside the layer for these shorter durations along the surface of the porosity network. On the contrary, in the case of brush application, the smaller amount of available solution seems to limit the penetration of the complexing agent within the corrosion layer. Moreover, the drying time between two applications can induce an evaporation of the solution before it penetrates. In conclusion to this part, comparing the efficiency of the different application modes the penetration of the solution through the corrosion layer is a key factor to enhance the quantity of the copper decanoate precipitated inside the corrosion layer.

3.4. Efficiency and durability of the treatments

All treated samples were immersed in a D₂O bath during 1 and 4 months (see methodological part) to compare the penetration of water. For each sample, a δ_D factor was evaluated by comparison with a blank sample. It can be first observed that the deuterium enrichment in the untreated sample increases sharply in function of the immersion time (3-fold higher after 4 months than after 1 month). This sharp increase, showing no damping even after 4 months (Figure 9) suggests that the pores are not saturated yet by water after four months immersion in D₂O. This could be linked to the presence of a nanoporous network, into which water penetrates more slowly. Looking closer at

treated samples, whatever the protection treatment is, the results show that the δ_D is significantly lower than without protection, especially after 4 months of immersion in D_2O for which the non-treated one presents a significant increase whereas the treated one are in the same order of range for one and four months of immersion. This decrease of water penetration for the treated samples is related to the presence of the wax or copper decanoate layers that are observed on all the treated samples, regardless the depth of the treatment penetration inside the corrosion layer. Nevertheless, looking closer to the δ_D values, the repellent behavior varies with the nature of the treatments and its application mode.

First for both waxed samples (Figure 10), we can observe after 1 month in D_2O a significant decrease of deuterium enrichments compared to the untreated sample. This decrease is even more important for the sample treated with “cold” wax (from 1400% for untreated sample to approximately 100% for the “cold” wax). We can also observe that the deuterium enrichment decreases for both application modes after 4 months in D_2O . For this duration, unlike a 1-month immersion, a less important difference is observed between “hot” and “cold” wax application (620 and 930% respectively). Moreover, the deuterium enrichment is the same for 1- and 4-month immersion in D_2O for the “hot” wax application but increases significantly for the cold wax application.

Whatever the immersion time in D_2O is, the deuterium enrichments for samples protected by the decanoic acid solution are all lower than the values for the untreated sample. After 1 month in D_2O the deuterium enrichment is similar for the treatment applied by brush or by immersion for 1 minute (respectively 800% and 700% for a value of 1300% without treatment). For immersion times of 30 minutes and 2 hours the deuterium enrichments is much less important (about 300%). After 4 months in D_2O the deuterium enrichments is of 3500% without treatment and is lowered to 1000% for the 1 minute in HC_{10} sample. This enrichment is even lower for the brush application or immersion times of 30 minutes and 2 hours and ranges between 420 and 700% in these cases.

Then, the durability of the protection treatments under external stresses as leaching due to rain was evaluated, again, by looking at the D_2O quantity that penetrates in the layer after leaching. No significant difference of δ_D value is observed between leached and non-leached samples for “hot” wax treatment (Figure 11a). At the contrary a difference of δ_D is observed between leached and non-leached samples protected by the “cold” wax treatment (Figure 11a). In this latter sample we showed previously that the wax coating is more superficial. It seems that the leaching deteriorates more rapidly its protectiveness properties than in the case of the “hot” treatment that shows a better resistance to degradation. A sharp difference of δ_D enrichment is also observed on the sample protected by decanoic acid applied by brush and submitted to leaching. That is not the case for the

one immersed one minute in HC₁₀, for which no difference of δ_D is measured for leached and non-leached samples (Figure 11b).

As shown previously, the amount of decanoic compounds is lower inside the corrosion layer in the case of the application by brush. It seems consequently that the penetration of the treatment significantly increases its durability.

4. Conclusion

In this study, the protectiveness of two treatments applied on long term corroded copper in atmosphere has been studied: a classical wax coating on one side and a green inhibitor, the decanoic acid on the other side. The aim of this work is to understand the physico-chemical processes occurring in order to ameliorate the use and protocols of application for cultural heritage metals. The methodology set up is based on

- the chemical characterization at the micrometric scale of the corrosion layers using SEM-EDX and μ Raman spectroscopy,
- the use of ¹³C detected by NRA to refine the knowledge about the decanoic acid interaction with the corrosion layer
- the use of deuterated water detected by ToF-SIMS to evaluate the protectiveness of a set of treated samples and of a set of treated and weathered ones.

For the non-treated samples the results highlight that the corrosion product layer is similar to the one observed on long term corroded copper samples, namely a thin inner layer of cuprite of few micrometers and a thicker outer layer of brochantite of several tenth micrometers.

For the treated samples the study shows that for both treatments by wax or decanoic acid the application mode affects its penetration into the corrosion layer. Indeed, regarding microcrystalline waxes, heating the substrate during application decreases the wax viscosity and then facilitates its penetration. For the decanoic acid solution an application by immersion considerably increases its penetration compared to the application by brush, leading to a greater conversion of brochantite to copper decanoate. The decrease in water penetration into the corrosion layer could be attributed to the conversion of corrosion products into copper decanoate.

The durability of a treatment under rain leaching appears to be related to the application mode. Indeed, these results showed that a protective treatment whose application mode allows a good penetration in the corrosion layer shows a better resistance under leaching.

Consequently this work brings new insights on one hand of the treatment penetration and on the other hand of the efficiency and durability of both treatments regarding the immersion time in water and the durability under leaching action.

Data availability

Data will be made available upon request.

Declaration of Competing Interest

The authors report no declarations of interest.

Acknowledgement

Labex PATRIMA and Fondation des Sciences du Patrimoine (EUR-17-EURE-0021) are thanked for supporting this study.

5. References

- [1] L. Robbiola, C. Fiaud, S. Pennec, New model of outdoor bronze corrosion and its implications for conservation, in: ICOM Comm. Conserv. Tenth Trienn. Meet., 1993: pp. 796–802.
- [2] S. Oesch, P. Heimgartner, Environmental effects on metallic materials—results of an outdoor exposure programme running in Switzerland, *Mater. Corros.* 47 (1996) 425–438.
- [3] S. Oesch, M. Faller, Environmental effects on materials: The effect of the air pollutants SO₂, NO₂, NO and O₃ on the corrosion of copper, zinc and aluminium. A short literature survey and results of laboratory exposures, *Corros. Sci.* 39 (1997) 1505–1530.
- [4] L.B. Brostoff, *Coating strategies for the protection of outdoor bronze art and ornamentation*, 2003.
- [5] G. D'Ercoli, M. Marabelli, V. Santin, A. Buccolieri, G. Buccolieri, A. Castellano, G. Palamà, Restoration and conservation of outdoor bronze monuments: diagnosis and non-destructive investigation, in: Proc. 9th Int. Conf. NDT Art, Notea, A., Ed., Hebr. Univ. Jerusalem Jerusalem, Isr., 2008: p. 30.
- [6] J.C.-V.J. Cama-Villafranca, The Metal Patina and Surface Layer of El Caballito: Calling

Things by Their Name, in: *Met. 2019 - Proc. Interim Meet. ICOM-CC Met. Work. Group; Neuchatel (CH), 2-6 Sept. 2019, 2019.*

- [7] K.P. FitzGerald, J. Nairn, G. Skennerton, A. Atrens, Atmospheric corrosion of copper and the colour, structure and composition of natural patinas on copper, *Corros. Sci.* 48 (2006) 2480–2509.
- [8] D. De la Fuente, J. Simancas, M. Morcillo, Morphological study of 16-year patinas formed on copper in a wide range of atmospheric exposures, *Corros. Sci.* 50 (2008) 268–285. <https://doi.org/10.1016/j.corsci.2007.05.030>.
- [9] A. Krättschmer, I.O. Wallinder, C. Leygraf, The evolution of outdoor copper patina, *Corros. Sci.* 44 (2002) 425–450.
- [10] X. Zhang, W. He, I.O. Wallinder, J. Pan, C. Leygraf, Determination of instantaneous corrosion rates and runoff rates of copper from naturally patinated copper during continuous rain events, *Corros. Sci.* 44 (2002) 2131–2151.
- [11] K. Nassau, A.E. Miller, T.E. Graedel, The reaction of simulated rain with copper, copper patina, and some copper compounds, *Corros. Sci.* 27 (1987) 703–719.
- [12] R. Picciochi, A.C. Ramos, M.H. Mendonça, I.T.E. Fonseca, Influence of the environment on the atmospheric corrosion of bronze, *J. Appl. Electrochem.* 34 (2004) 989–995.
- [13] M. Wadsak, T. Aastrup, I. Odnevall Wallinder, C. Leygraf, M. Schreiner, Multianalytical in situ investigation of the initial atmospheric corrosion of bronze, *Corros. Sci.* 44 (2002) 791–802.
- [14] F. Ospitali, C. Chiavari, C. Martini, E. Bernardi, F. Passarini, L. Robbiola, The characterization of Sn-based corrosion products in ancient bronzes: a Raman approach, *J. Raman Spectrosc.* 43 (2012) 1596–1603.
- [15] E. Bernardi, C. Chiavari, C. Martini, L. Morselli, The atmospheric corrosion of quaternary bronzes: An evaluation of the dissolution rate of the alloying elements, *Appl. Phys. A Mater. Sci. Process.* 92 (2008) 83–89.
- [16] C. Chiavari, E. Bernardi, A. Balbo, C. Monticelli, S. Raffo, M.C. Bignozzi, C. Martini, Atmospheric corrosion of fire-gilded bronze: corrosion and corrosion protection during accelerated ageing tests, *Corros. Sci.* 100 (2015) 435–447. <https://doi.org/https://doi.org/10.1016/j.corsci.2015.08.013>.
- [17] L. Robbiola, K. Rahmouni, C. Chiavari, C. Martini, D. Prandstraller, A. Texier, H. Takenouti, P. Vermaut, New insight into the nature and properties of pale green surfaces of outdoor bronze monuments, *Appl. Phys. A Mater. Sci. Process.* 92 (2008) 161–169.
- [18] G. Masi, J. Esvan, C. Josse, C. Chiavari, E. Bernardi, C. Martini, M.C. Bignozzi, N. Gartner,

- T. Kosec, L. Robbiola, Characterization of typical patinas simulating bronze corrosion in outdoor conditions, *Mater. Chem. Phys.* 200 (2017) 308–321. <https://doi.org/10.1016/j.matchemphys.2017.07.091>.
- [19] T.E. Graedel, Copper patinas formed in the atmosphere-II. A qualitative assessment of mechanisms, *Corros. Sci.* 27 (1987) 721–740.
- [20] D. Knotkova, K. Kreislova, Atmospheric corrosion and conservation of copper and bronze, *Environ. Deterior. Mater.* 21 (2007) 107.
- [21] D.W. Rice, P. Peterson, E.B. Rigby, P.B.P. Phipps, R.J. Cappell, R. Tremoureux, Atmospheric corrosion of copper and silver, *J. Electrochem. Soc.* 128 (1981) 275–284.
- [22] J.P. Franey, M.E. Davis, Metallographic studies of the copper patina formed in the atmosphere, *Corros. Sci.* 27 (1987) 659–668.
- [23] M. Morcillo, T. Chang, B. Chico, D. de la Fuente, I. Odnevall Wallinder, J.A. Jiménez, C. Leygraf, Characterisation of a centuries-old patinated copper roof tile from Queen Anne's Summer Palace in Prague, *Mater. Charact.* 133 (2017) 146–155.
- [24] E. Cano, D. Lafuente, 26 - Corrosion inhibitors for the preservation of metallic heritage artefacts, in: P. Dillmann, D. Watkinson, E. Angelini, A.B.T.-C. and C. of C.H.M.A. Adriaens (Eds.), *Eur. Fed. Corros. Ser.*, Woodhead Publishing, 2013: pp. 570–594.
- [25] T. Kosec, H.O. Čurković, A. Legat, Investigation of the corrosion protection of chemically and electrochemically formed patinas on recent bronze, *Electrochim. Acta.* 56 (2010) 722–731.
- [26] E. Joseph, P. Letardi, R. Mazzeo, S. Prati, M. Vandini, Innovative treatments for the protection of outdoor bronze monuments, in: *Proc. Interim Meet. ICOM-CC Met. WG*, Amsterdam, Netherlands, 2007: p. 7177.
- [27] P. Letardi, Laboratory and field tests on patinas and protective coating systems for outdoor bronze monuments, in: *Proc. Int. Conf. Met. Conserv. Canberra, Aust.*, 2004: p. 379387.
- [28] L.A. Ellingson, T.J. Shedlosky, G.P. Bierwagen, E.R. de la Rie, L.B. Brostoff, The use of electrochemical impedance spectroscopy in the evaluation of coatings for outdoor bronze, *Stud. Conserv.* 49 (2004) 53–62.
- [29] P. Letardi, R. Spiniello, Characterisation of bronze corrosion and protection by contact-probe electrochemical impedance measurements, in: *Met. 2001 Proc. Int. Conf. Met. Conserv. Santiago, Chile, 2-6 April 2001*, Western Australian Museum, 2004: pp. 316–319.
- [30] C. Price, D. Hallam, G. Heath, D. Creagh, J. Ashton, An electrochemical study of waxes for bronze sculpture, in: *Conférence Int. Sur La Conserv. Des Métaux*, 1997: pp. 233–241.
- [31] V. Otieno-Alego, G. Heath, D. Hallam, D. Creagh, Electrochemical evaluation of the anti-

- corrosion performance of waxy coatings for outdoor bronze conservation, in: *Conférence Int. Sur La Conserv. Des Métaux*, 1998: pp. 309–314.
- [32] V. Otieno-Alego, D. Hallam, A. Viduka, G. Heath, D. Creagh, Electrochemical impedance studies of the corrosion resistance of wax coatings on artificially patinated bronze, in: *Conférence Int. Sur La Conserv. Des Métaux*, 1998: pp. 315–319.
- [33] S. Goidanich, L. Toniolo, S. Jafarzadeh, I.O. Wallinder, Effects of wax-based anti-graffiti on copper patina composition and dissolution during four years of outdoor urban exposure, *J. Cult. Herit.* 11 (2010) 288–296.
- [34] A. Texier, A.-M. Geffroy, D. Syvilay, T. Brocard-Rosa, Les cires microcristallines dans la protection de la stauaire en cuivre et alliages de cuivre exposée en extérieur, in: *Métal à Ciel Ouvert - 15es Journées d'étude La SFIIC - ICOMOS Fr.*, Paris, 2014.
- [35] B.H. Madsen, A preliminary note on the use of benzotriazole for stabilizing bronze objects, *Stud. Conserv.* 12 (1967) 163–167.
- [36] X. Wu, N. Chou, D. Lupher, L.C. Davis, Benzotriazoles: Toxicity and Degradation, *Conf. Hazard. Waste Res.* (1998) 374–382.
- [37] D. Pillard, J. Cornell, D. Dufresne, M. Hernandez, Toxicity of Benzotriole and Benzotriazole Derivatives to three Aquatic Species, *Water Res.* 35 (2001) 557–560.
- [38] M. Albin, P. Letardi, L. Mathys, L. Brambilla, J. Schröter, P. Junier, E. Joseph, Comparison of a bio-based corrosion inhibitor versus benzotriazole on corroded copper surfaces, *Corros. Sci.* 143 (2018) 84–92.
- [39] S. Hollner, F. Mirambet, E. Rocca, S. Reguer, Evaluation of new non-toxic corrosion inhibitors for conservation of iron artefacts, *Corros. Eng. Sci. Technol.* 45 (2010) 362–366.
- [40] S. Hollner, F. Mirambet, A. Texier, E. Rocca, J. Steinmetz, Development of new non-toxic corrosion inhibitors for cultural property made of iron and copper alloys, in: *Strateg. Sav. Our Cult. Heritage. Proc. Int. Conf. Conserv. Strateg. Sav. Indoor Met. Collect. Cairo*, 2007: pp. 156–161.
- [41] G. Rapp, C. Degriigny, F. Mirambet, S. Ramseyer, A. Tarchini, The application of non-toxic corrosion inhibitors for the temporary protection of iron and copper alloy in uncontrolled environments, *Metal.* (2010) 185–190.
- [42] E. Rocca, G. Bertrand, C. Rapin, J.C. Labrune, Inhibition of copper aqueous corrosion by non-toxic linear sodium heptanoate: mechanism and ECAFM study, *J. Electroanal. Chem.* 503 (2001) 133–140.
- [43] C. Degriigny, V. Argyropoulos, P. Pouli, M. Grech, K. Kreislova, M. Harith, F. Mirambet, N. Hadad, E. Angelini, E. Cano, The methodology for the PROMET project to develop/test new

non-toxic corrosion inhibitors and coatings for iron and copper alloy objects housed in Mediterranean museums, in: *Met. 07. Proc. Interim Meet. ICOM-CC Met. WG, 2007*: pp. 31–37.

- [44] S. Hollner, Développement de nouveaux traitements de protection à base d'acide carboxylique pour La conservation d'objets en fer du patrimoine culturel, These. UHP Nancy (2009).
- [45] E. Rocca, F. Mirambet, P. Dillmann, M. Folzan, S. Reguer, Protection treatments based on derivatives of vegetable oils for iron corroded object: the case of thick corrosion layers, (2012) 120–125.
- [46] C. Rapin, P. Steinmetz, J. Steinmetz, Etude de l'inhibition de la corrosion aqueuse du cuivre par les carboxylates linéaires saturés. I. Pouvoir inhibiteur des carboxylates linéaires de formule $\text{CH}_3(\text{CH}_2)_n\text{-2COONa}$, *Rev. Métallurgie*. 93 (1996) 281–290.
- [47] C. Rapin, A. D'huysser, J.-P. Labbe, L. Gengembre, P. Steinmetz, Etude de l'inhibition de la corrosion aqueuse du cuivre par les carboxylates linéaires saturés.-II. Caractérisation des films superficiels formés par réaction entre le cuivre et l'anion heptanoate, *Rev. Métallurgie*. 93 (1996) 719–727.
- [48] I. Milošev, T. Kosec, M. Bele, The formation of hydrophobic and corrosion resistant surfaces on copper and bronze by treatment in myristic acid, *J. Appl. Electrochem*. 40 (2010) 1317–1323.
- [49] D. Syvilay, Evaluation des systèmes de protection pour la statuaire en cuivre exposée en extérieur, (2011).
- [50] C.R. Wilke, P. Chang, Correlation of diffusion coefficients in dilute solutions, *AIChE J.* 1 (1955) 264–270.
- [51] A. Kratschmer, I. Wallinder, C. Leygraf, The evolution of out copper patina, *Corros. Sci.* 44 (2002) 425–450.
- [52] L. Robinet, M.-C. Corbeil, The Characterization of Metal Soaps, *Stud. Conserv.* 48 (2003) 23–40.
- [53] P. Berger, G. Revel, Microsonde nucléaire: principe et appareillage, *Tech. l'ingénieur. Anal. Caractérisation*. (2005).
- [54] H. Khodja, E. Berthoumieux, L. Daudin, J.-P. Gallien, The Pierre Süe Laboratory nuclear microprobe as a multi-disciplinary analysis tool, *Nucl. Instruments Methods Phys. Res. Sect. B Beam Interact. with Mater. Atoms*. 181 (2001) 83–86.
- [55] M. Mayer, SIMNRA user's guide, (1997).
- [56] G. Socrates, Infrared and Raman characteristic group frequencies: tables and charts, John Wiley & Sons, 2004.

- [57] I.O. Wallinder, C. Leygraf, A study of copper runoff in an urban atmosphere, *Corros. Sci.* 39 (1997) 2039–2052.
- [58] T. Chang, I. Odnevall Wallinder, D. de la Fuente, B. Chico, M. Morcillo, J.-M. Welter, C. Leygraf, Analysis of Historic Copper Patinas. Influence of Inclusions on Patina Uniformity, *Materials (Basel)*. 10 (2017) 298.
- [59] W. He, I.O. Wallinder, C. Leygraf, A laboratory study of copper and zinc runoff during first flush and steady-state conditions, *Corros. Sci.* 43 (2001) 127–146.
- [60] F. Gao, A.A. Sonin, Precise deposition of molten microdrops: the physics of digital microfabrication, *Proc. R. Soc. Lond. A.* 444 (1994) 533–554.

Captions

Figures

Figure 1: Metal micrograph of a copper sample from the roof of the St Martin church, Metz

Figure 2: Raman spectra of brochantite, cuprite, copper decanoate, Cosmolloïd wax and decanoic acid

Figure 3: EDX maps of copper ($K\alpha$), oxygen ($K\alpha$), sulfur ($K\alpha$) and chlorine ($K\alpha$) of the corrosion layer of copper sample from St Martin church, Metz

Figure 4: optical image of the layer and corresponding μ Raman maps of cuprite (red, ROI 216 cm^{-1}) and brochantite (green, ROI 973 cm^{-1}) (a); average Raman spectra of the outer (b) and inner (c) layers of copper sample from St Martin church, Metz

Figure 5: Thickness measurements of the corrosion layers of copper sample from St Martin church, Metz

Figure 6: Optical images and μ Raman maps of cuprite (red, ROI 216 cm^{-1}), brochantite (green, ROI 973 cm^{-1}) and Cosmolloïd wax (magenta, ROI 1061 cm^{-1}); average Raman spectra of the inner and outer layers of copper samples from St Martin church, Metz, treated with Cosmolloïd wax by “hot” (a) and “cold”(b) application

Figure 7: μ Raman maps of cuprite (red, ROI 216 cm^{-1}), brochantite (green, ROI 973 cm^{-1}) and copper decanoate (blue, ROI 290 cm^{-1}); average Raman spectra of the inner and outer layers of copper samples from St Martin church, Metz, treated with decanoic acid applied with a brush (a) and by immersion for 1h (b) and 3h (c)

Figure 8: Carbon-13 enrichments as a function of immersion time in $\text{H}^{13}\text{C}_{10}$ (the red cross is the carbon-13 enrichment for $\text{H}^{13}\text{C}_{10}$ applied with a brush in 2 layers)

Figure 9: Deuterium enrichments as a function of immersion time in D_2O

Figure 10: Deuterium enrichments in the corrosion layers for the untreated sample (grey), the waxed samples (orange) and the copper samples from St Martin church, Metz, treated with HC_{10} (blue), after 1 month (left) and 4 months (right) in D_2O

Figure 11: Deuterium enrichments in the corrosion layers of samples with Cosmolloïd wax (a) and decanoic acid (b), without and with leaching solicitation